A STRUCTURAL AND FUNCTIONAL ANALYSIS OF *NEMATOSTELLA VECTENSIS* MAJOR INTRINSIC PROTEINS

By

Jonathon C. Taylor

A thesis submitted to the faculty of
The University of North Carolina at Charlotte
in partial fulfillment of the requirements
for the degree of Master of Science in
Biological Sciences

Charlotte

2020

Approved by:

_____
Dr. Richard Chi

_____
Dr. Adam Reitzel

_____
Dr. Andrew Truman

ABSTRACT

JONATHON C. TAYLOR. A structural and functional analysis of *NEMATOSTELLA VECTENSIS* major intrinsic proteins. (Under the direction of Dr. RICHARD CHI and DR. ADAM REITZEL)

There is currently a major gap in understanding the physiological processes of tissue grade animals from early diverging phyla, particularly within the context of the molecular mechanisms in response to osmotic variation. A key protein family essential for the regulation of intracellular water and solute concentrations are the Major Intrinsic Proteins (MIPs), these include aquaporins (Aqps) and aquaglyceroporins (Glps). Here, we report the identification and functional analysis of MIPs in *Nematostella vectensis*, a member of the phylum Cnidaria that represents a unique group of tissue grade organisms. Using a combination of sequence similarity and phylogenetic analyses, we successfully identified eight MIPs in *N.vectensis*, 4 Aqps, 3 Glps, and 1 in the atypical MIP groups 11/12. Putative MIPs were recombinantly expressed in budding yeast, *Saccharomyces cerevisiae*, and tested for functionality under osmotic stress. *N. vectensis* MIPs displayed varying degrees of functionality, ranging from no effect indicating lack in functionality to lethality indicating MIP functional capacity to translocate water, suggesting a phylogenetic approach paired with an *in vivo* functionality assay is critical for their characterization. Total *N. vectensis* MIP transcripts were also quantified during acute and long-term salinity exposure that support the results from the yeast experiments. Furthermore, based on high confidence protein structure homology modeling, we demonstrate a significant correlation between three biophysical pore properties that accurately predict functionality. The identification and functional analysis of these MIPs suggest a high degree of diversification at the cnidarian-bilaterian ancestor both in terms of number and function.

ACKNOWLEDGEMENTS

I would like to thank my committee members Dr. Richard Chi, Dr. Adam Reitzel and Dr. Andrew Truman. Dr. Chi was instrumental in guiding me through my thesis research. Dr. Chi provided me with the skills to perform some of the most fundamental techniques in cell and molecular biology. Moreover, Dr. Chi guided me as a student and allowed me to develop myself and understand what is truly meaningful to me as I now continue to work toward a career in medicine. Dr. Chi gave me the confidence I needed to pursue my newfound goals and has allowed me to grow as a more refined student of science. Dr. Reitzel was instrumental in making this experience enlightening by exposing me to the diversity and interdisciplinary nature of biology. Dr. Reitzel provided me with a greater appreciation for evolutionary biology and revealed a deeper complexity to all of the fundamental questions that science has to offer. Dr. Reitzel's lab also provided the background data and cDNA necessary to begin this investigation into structure and function of *N. vectensis* MIPs. I would also like to thank Vanna Sombatsaphay who, as a graduate student under Dr. Reitzel, performed *in vivo* transcriptional analysis of *N. vectensis* MIPs which served to make a complete and cohesive story to understand the results in this investigation. Dr. Truman was an excellent mentor who provided invaluable instruction on how to approach questions in science through established methodologies. Dr. Truman was always an enthusiastic and available resource helping me through this process.

TABLE OF CONTENTS

LIST OF TABLES

LIST OF FIGURES

LIST OF ABBREVIATIONS

Aqp	Aquaporin
Glp	Aquaglyceroporin
MIP	Major Intrinsic Protein
ANOVA	Analysis of Variance
PCR	Polymerase Chain Reaction
OD	Optical Density
SDS-PAGE	Sodium Dodecyl Sulfate Polyacrylamide Gel Electrophoresis
PDB	Protein Data Bank
I-TASSER	Iterative Threading Assembly Refinement

CHAPTER 1: INTRODUCTION

Variability in environmental salinity requires organisms to have efficient mechanisms to respond to changes in the osmotic environment. These molecular mechanisms result in the physiological plasticity that is commonly observed in animals. Areas such as coastal aquatic habitats have strong variations in salinity that requires resident species to have broad physiological tolerances. The variation in salinity (and other abiotic factors) is further exacerbated by global climate change which can precipitate broad changes in food web stability [1,2,3]. Estuaries are typified by wide fluctuations of abiotic conditions such as temperature and salinity, which are interrelated due to evaporated loss and intense episodic rainfall. Thus, estuaries, like other coastal zones, are particularly susceptible to global climate change because of the lower capacity for buffering of shallow waters and exchanges with air, land, and fresh waters that predispose these habitats to extreme variation in salinity and other abiotic conditions [4].

Many organisms have been studied with regard to osmoregulation and typically exhibit unique compensatory strategies to placate osmotic stress. *Fundulus heteroclitus* (killifish) exhibit the unique strategy of osmoregulation via ion transport through the gills, altering seawater and freshwater ingestion, as well as having developed adaptation within the kidneys [5,6]. *Artemia salina* (brine shrimp) maintains the ability to encyst to avoid drying, maintaining dedicated salt glands, and surrounding itself by a cuticle [7,8]. While most osmoregulation research strategies have centered on crustaceans or vertebrates, information on tissue grade organisms (e.g., cnidarians, ctenophores, acoels) from early diverging phyla is lacking, creating a major gap in the field. These organisms rely on cellular level regulatory mechanisms such as proteins facilitating water movement across their membranes instead of specialized organelles or internal

body fluids and are particularly interesting because some species in each group specialize in habitats that are highly variable environments. Our study is the first to investigate a phylogenetic comparison of a membrane protein diversification and their role in cnidarians.

1.1 *Nematostella vectensis* is a Representative of the Early Diverging Phyla.

Nematostella vectensis was selected for this study because it is native to the Atlantic coast of the US and Canada and resides in brackish habitats (9‰ to 51‰), such as tidal pools of salt marshes [9, 10,11]. Similar to many estuarine organisms, this species is tolerant of a wide range of temperature and other environmental variables (e.g., salinity, oxygen concentration), which correlates with its distribution in high marsh habitats, and previous studies have suggested this tolerance resulted due to adaptation [9,10,12]. *N. vectensis* is also a model for comparative genomics due to the availability of a sequenced genome [13]. After the initial release of the genome in 2007, extensive sequencing of transcriptomes from developmental stages and sequencing of chromatin-immunoprecipitation promoter elements have resulted in a well annotated genome [14,15]. Additionally, *N. vectensis* has developed into an excellent model system for molecular and developmental biology because it is easily cultured in the laboratory to produce high populations [16, 17] and individuals can also be cultured on a weekly cycle to induce production of gametes for embryos generation [18-20]. Therefore, *N. vectensis* creates a unique opportunity to thoroughly study the diversity, evolutionary history, molecular biology, and function of MIPs. Taken together, *N. vectensis* is an ideal representative of early diverging phyla to determine how MIP variation may be functionally tied to phenotypic variation in molecular or physiological traits due to environmental change.

1.2 Structure and Function of Major Intrinsic Proteins

In contrast to larger, charged molecules, water is recognized as having a unique capacity to facilitate passive movement through lipid bilayers with relatively good efficiency. However, how protein mediation of water transport across membranes is not fully understood [21]. The proteins that are responsible for water transport are aquaporins (Aqps) and aquaglyceroporins (Glps). These proteins, as well as other closely related 'atypical aquaporins', constitute an essential, ancient, monophyletic and conserved group of proteins known as Major Intrinsic Proteins. These molecules are critical in the homeostatic regulation of intracellular environments and have been shown to mitigate osmotic irregularities [22].

Aqps and Glps function similarly for water transport but also have many fundamental distinctions. While each can be recognized through their homotetrameric quaternary structures and their capacity to facilitate the movement of water across membranes, a molecular selectivity filter, or the narrowest region through the transmembrane pore, provide a clear differentiation. For example, the selectivity filter of *E. coli* aquaporin Z is slightly smaller (1.1 Å) than that of aquaglyceroporin (1.7 Å) as well as being more hydrophilic. These differences in size and hydropathy explain their respective capacities to shuttle only water or both water and solutes across membranes. The filter itself, which consists of F43, H174, T183, and R189, has been examined with *E. coli* aquaporin Z protein (AqpZ) and was identified as a key region to focus this study on (Fig. 1) [23].

There have been some elucidations regarding the diversity and emergence of subgroups of MIPs precipitated by independent studies which have successfully categorized subgroups for each Aqp or Glp lineage, however further genomic analysis is needed to broaden an understanding of existing subgroups [24,25]. Previous studies of MIPs have revealed that there is

not necessarily a universal conservation of each group since classical aquaporins are absent in some organisms such as the sponge [26].

1.3 *Saccharomyces cerevisiae* is a Useful Tool to Evaluate Major Intrinsic Protein Function.

In recent years, others in the field have successfully utilized budding yeast to determine the transport properties for human MIPs. This was achieved through heterologous expression in yeast, using yeast fitness assays to determine whether MIPs transport water and small solutes (urea, glycerol) [27]. Interestingly, yeast have four proteins belonging to the aquaporin family, two orthodox aquaporins (Aqy1 and Aqy2) and two aquaglyceroporins (Fps1 and Ylf054c). However, in laboratory strains orthodox aquaporins have incurred spontaneous mutations rendering them nonfunctional, leaving only Fps1 and Ylf054c to facilitate osmoregulation [28]. The pathways to combat hyperosmotic shock in yeast are also well defined and typically, yeast cells can tolerate increased osmotic conditions by accumulating glycerol via Gdp1 and Gpp2 encoding enzymes involved in the glycerol biosynthetic pathway [29, 30]. It is worth noting that previous studies using yeast to understand MIP function typically mitigate this compensatory mechanism by using yeast ablated for GPD1 or GPD2 in order to see a change in growth fitness. The rationale being that upon the addition of a functional foreign MIP, regulatory mechanisms fail, and in the presence of high osmotic stress, water expels out of the cell through osmosis leading to reduced cell fitness (Fig. 2). Functionality is also partly determined by subcellular localization to the plasma membrane. Proper MIP insertion into the plasma membrane is an indication that their complex tertiary structures are achievable *in vivo* and can be properly trafficked. Taken together, yeast can provide a powerful assay for determining MIP functionality.

1.4 Protein Structure May Indicate MIP Functionality.

Given the expansive database of protein structures available, evaluating and defining the biological function of MIPs using structural-based approaches is now feasible [31, 32]. Previously, the subatomic structures of *E. coli* AqpZ and GlpF were solved using X-ray crystallography. This provides a high-resolution template to determine the structure and function for similar proteins in *N. vectensis* using protein homology building. Therefore, high confidence protein homology models can be built, and their structures can be analyzed to predict functionality. We hypothesize this approach can assist in determining the selectivity filters of each *N. vectensis* MIP and provide insight into how these organisms can operate within the context of their variable habitats.

CHAPTER 2: MATERIALS AND METHODS

2.1 Bacterial Transformation and Growth Conditions

Competent *E. coli* were mixed with 3 µL of donor or destination vector. The mixture was iced for 30 minutes, heat shocked at 42°C for 30 seconds followed by 2 minutes on ice. 500 µL of room temperature SOC media was added and the bacteria were incubated at 37 °C for 1 hour with shaking. Bacteria were then plated on Luria Broth (LB) media containing 50 µg/mL of appropriate antibiotic selection.

2.2 Yeast Growth Conditions

S. cerevisiae BY4742 strains were grown in YPD media containing 2% peptone, 1% yeast extract and 2% dextrose added after autoclaving. Yeast requiring selection were grown in dropout media containing 0.67% YNB without amino acids, 0.077% complete supplement mixture minus uracil, and 2% dextrose. Growth assay plates were made similarly with dropout media with the indicated concentrations of NaCl, KCl, and sorbitol dissolved, respectively.

2.3 Generation of Expression Vectors and Yeast Strains

The *S. cerevisiae* strain used in this investigation was BY4742 (genotype: MATα his3Δ1 leu2Δ0 lys2Δ0ura3Δ0) [33]. *gpd1Δ* mutants were created using standard homologous recombinant techniques [34]. Plasmids containing *N. vectensis* full length MIP genes (see Table 1 for primers) were used to PCR amplify each MIP gene for yeast expression. The original PCRs used cDNA libraries prepared from RNA from multiple developmental stages (embryos, larvae, juveniles) and adults. Forward and reverse primers were designed with complementary sequences to the beginning and ending of the gene with the addition of attB sites flanking the gene on either side (Table 1). Gateway cloning was performed to shuttle these PCR amplified *N. vectensis* MIPs into Gateway™ pDONR™221 Vectors and subsequently isolated, purified and

transferred into pAG426GPD-ccdB-EGFP destination vectors [35]. After generating each destination vector, *gpd1Δ* strains were individually transformed with one of the seven MIP-containing destination vectors or empty pAG426GPD-ccdB-EGFP vector using LiAcetate [34]. BP and LR reactions were performed using established protocols obtained from the A. Untergasser lab [36]. Aqp6 was not successfully amplified and thus will not be reported in this thesis.

2.4 Survival Growth Assay

Overnight cultures were grown in C-URA liquid media and harvested at OD_{600} ~ 0.6-0.8. Cells were resuspended to 2.5 ODs and 120 µL of each strain were added to the first well of a sterile 96 well plate. Neighboring wells were diluted with 100 µL of sterile water. 20 µL of cells was diluted into each additional well and spotted onto C-URA plates containing indicated solutes. Plates was grown at 30 °C for 3-5 days. Each assay was repeated 3-5 times and the most representative plates from each condition are shown.

2.5 Quantitative Western Blot Analysis

Yeast expressing indicated expression vectors were grown to logarithmic phase (OD_{600} ~ 0.6) and centrifuged at 3400 rpm for 4 minutes. The resulting pellet was washed with 500 mL of water and centrifuged at 8000 rpm for 1 minute. The supernatant was removed, and the pellet was frozen at -80 °C prior to the addition of 120 µL of protein loading buffer (10% SDS, 500 Mm DTT, 50% glycerol, 500 mM Tris-HCl, and 0.05% bromophenol blue dye). 50-100 µL of zirconium beads were added and the cells were placed in a gene disruptor for 1 minute. All samples were denatured at 95 °C and centrifuged at max speed for 1 minute. The supernatant was loaded onto SDS-PAGE and transferred onto nitrocellulose. Blots were blocked with PBS-5% milk solution for 1 hour and then incubated with a 1:5000 diluted anti-GFP mouse

monoclonal antibody. The membrane was then washed and incubated with a 1:10000 dilution of goat anti-mouse HRP-conjugated secondary antibody. For Pgk1 blots, membranes were stripped and anti-Pgk1 mouse monoclonal antibody was added at 1:5000 dilution. Quantitative densitometric analysis was completed with BIO-RAD Image Lab 6.1 and is shown as a summation of 2-3 experiments. A single factor ANOVA was performed to determine significance ($p=0.05$).

2.6 Live-Cell Fluorescence Microscopy

MIP localization was performed using live-cell fluorescence deconvolution microscopy. Overnight cultures of yeast strains expressing *N. vectensis* MIPs were grown at 30 °C to OD_{600} ~ 0.6-0.8. The samples were captured using a GE-DeltaVision workstation with a standard DAPI/FITC/TRITC/Cy5 filter set. Images were taken at room temperature and Z-stack images were generated and deconvolved. Image analyses were completed using ImageJ v1.51.

2.7 Transcriptional Regulation of *N. vectensis* MIPs

Adult and larval *N. vectensis* were cultured under conditions of salinity stress and analyzed to characertize modulation in MIP transcription. For the adults, *N. vectensis* polyps were grown in a common garden condition (15ppt salinity, standard estuary) for >30 days. After this standardization condition, polyps were allocated into three replicate bowls to various different salinities or durations of exposure. To evaluate the impact of an acute shift in salinity on the expression level of MIPs, *N. vectensis* were shifted from a 15ppt saline environment to 5ppt, 15ppt, or 35ppt salinity conditions for a 6-hour duration. The difference in MIP expression following a shift in salinity was also observed in a chronic exposure context where adults were cultured at 5ppt and 35 ppt for 30 days. Chronic exposure conditions are denoted as 5-L and 35-L, where “L” indicates “long”. Following exposure, 2-3 *N. vectensis* adults from each replicate

bowl were preserved in RNA later until extractions were completed. For the larval stage, *N. vectensis* adults were spawned using a standard protocol to induce gametogenesis at 15ppt. Following release of gametes and fertilization, embryos were cultured at 15ppt for 4 days where they reached the larval stage. Larvae were then aliquoted into 4 replicate bowls for 3 salinity conditions: 15ppt (control), 5ppt, and 35ppt. Larvae were cultured at these salinities for 6-hours. At the end of the exposure, larvae were concentrated into 1.5 ml microcentrifuge tubes, flash frozen in liquid nitrogen, and stored at -80°C until extraction of RNA.

Total RNA was extracted from adult and larval samples using the Aurum™ Total RNA Fatty and Fibrous Tissue Kit (BioRad) with on-column DNAse treatment. RNA concentration was quantified with a NanoDrop (Thermo Scientific). 500 ng of total RNA was used as input for a 20 μL cDNA synthesis reaction using the iScript™ cDNA Synthesis Kit (BioRad) with recommended protocols. RT-qPCR was performed for each of the *N. vectensis* MIPs using the same approach for each gene and followed previously published protocols [37]. Briefly, oligonucleotide primers (see Table 1) were designed to amplify each *N. vectensis* MIP. Primers were 19-21 nucleotides, with a GC content of 40-60%, either overlapped predicted exon-exon boundaries by 3-4 bp or spanned a large intron and produced predicted amplicons of 78-115 bp with minimal predicted secondary structure (m-fold). A standard curve was constructed from serially-diluted plasmids containing the amplicon of interest. The standard curve was used in qPCR reactions to quantify amplification efficiency and to calculate the number of molecules per reaction. qPCR was performed using SsoFast EvaGreen Supermix (Bio-Rad), and reactions were run on a 7500 Fast Real Time PCR system (Applied Biosystems). For each gene, standards were run in duplicate wells and experimental samples were run in individually on a single plate. The PCR mixture consisted of 11.5 μL of molecular biology grade distilled water, 12.5 μL of SsoFast

EvaGreen Supermix, 0.5 μL of each gene-specific primer, and 1 μL of cDNA. PCR conditions were as follows: 95°C for 3 min; 40 cycles of 95°C for 15 s and 60°C for 45 seconds.The number of molecules per μL for each gene was calculated by comparing the threshold cycle (Ct) from the sample with the standard curve. Statistical analysis was performed via single factor ANOVA with a post hoc Tukey's honest significant difference test. A cut-off value of $p=0.05$ was used for statistical comparisons.

2.8 Protein Structure Homology Modeling

To produce each homology model, each MIP's primary amino acid sequence was entered into I-TASSER, using AqpZ as the template; the model with the highest confidence score was selected for each MIP and analyzed with MOLEonline [38,39]. Each resulting Protein Data Bank (PDB) file was evaluated using MOLEonline and pores models were generated. Using pore mode, beta structures and membrane regions were turned off and the probe radius was set to 13 and interior threshold was set to 0.3. Upon the generation of multiple transmembrane pores, we selected paths that utilized the entirety of the transmembrane region. Radius, hydropathy, and length of the selectively filter (SF) were also obtained from these models.

SF length (L) was defined as inversely proportional to aquaporin function and SF radius (r) was defined as proportional. The hydropathy of AqpZ (H_z) was used as a baseline for functionality and was subtracted from the hydropathy of *N. vectensis* MIPs (H_a) resulting in a hydropathy score. Subsequent hydropathy scores were multiplied by the ratio of the SF diameter and radius to obtain functionality scores. Functionality scores were baselined to AqpZ's functionality score of 0, with negative values (green) indicating a higher degree of functionality and positive values (red) indicating a lesser degree of functionality.

CHAPTER 3: RESULTS

3.1 Phylogenetic Analysis Reveals the Presence of Classical Aquaporins and Aquaglyceroporins in *N. vectensis*

We used a phylogenetic approach to predict MIPs in *N. vectensis*. Our results indicated there are three clades including aquaporin 1-like classical aquaporin, aquaporin 8, which is found only within the mitochondria, and aquaporin-3 like aquaglyceroporins. A maximum likelihood analysis of these aquaporins suggests *N. vectensis* has four classical aquaporins Aqp1, Aqp2, Aqp3, and Aqp4 and four aquaglyceroporins Aqp4, Aqp5, Aqp6, and Aqp8, and is lacking any proteins in the aquaporin-8 clade (Fig. 3). It is also worth noting an additional MIP that does not fit within any of the indicated clades, Aqp12 is also present. The presence of both classical aquaporins and aquaglyceroporins in *N. vectensis* suggests that aquaglyceroporin diversification occurred preceding the cnidarian-bilaterian ancestor. mRNA was isolated, and cDNA was obtained for each MIP. As noted in the Methods, Aqp6 was notsuccessfully amplified and thus was not cloned into yeast expression vectors.

3.2 *N. vectensis* MIPs Display Varying Functionality when Heterologously Expressed in Yeast.

In order to determine *N. vectensis* MIP function, we used standard yeast growth assay to evaluate MIP function [27]. Because standard laboratory yeast strains have developed loss of function mutations in their two orthodox aquaporin proteins, osmoregulatory is solely achieved by intracellular accumulation of glycerol via the GPD1/GPD2 pathway [27]. Therefore, query strains required ablation of GPD1 in addition to a heterologous expressing MIP to see plasmolysis phenotypes. Therefore, we expressed each *N. vectensis* MIP in yeast ablated for GPD1. The remaining seven MIPs were cloned into yeast expression vectors as C-terminal GFP fusion proteins and transformed into wildtype and *gpd1Δ* cells including strains with empty

vectors. A reduction in cell fitness under each condition of osmotic shock (0.5M NaCl, 0.5M KCl, and 0.8M sorbitol) was apparent only when Aqp1, Aqp4, Aqp5, and Aqp8 were expressed, with the most prominent phenotype occurring at 0.5 M NaCl (Fig. 4). This suggests Aqp1, Aqp4, Aqp5, Aqp8 are functional and under hypertonic stress overall fitness is reduced, likely due to water shuttling out of the cell upon exposure to osmotic stress. Aqp2, Aqp3, Aqp12 are likely not actively transporting water.

3.3 Quantitative Western Blot Analysis of *N. vectensis* MIPs Ectopically Expressed in *S. cerevisiae.*

Next, we sought to determine if MIP expression levels could explain the differences observed for functionality. Using quantitative western blot analysis, we successfully detected protein expression for each MIP, with each having varying degrees of expression (Fig. 5). Aqp1, Aqp3, and Aqp4 were found to be the highest expressing MIPs, while Aqp12 expression was minimal. Interestingly, we found no clear correlation between protein expression and functionality (Fig. 5).

3.4 *N. vectensis* MIPs Localize to the Plasma Membrane and Intracellular Compartments.

While total protein expression did not appear to influence functionality in yeast, it did not rule out that our constructs were misfolded or werenot trafficked correctly to the plasma membrane (PM) as others have seen using a yeast expression system [40]. Using live-cell fluorescence microscopy we localized each *N. vectensis* MIP. However, each MIP exhibited partial PM localization and decorated as expected, internal structures that appear to be the endomembrane system organelles such as the cortical ER, endosome and vacuole (Fig. 6). This suggests that each *N. vectensis* MIP can achieve proper tertiary structure and be trafficked correctly to the plasma membrane.

3.5 Transcriptional Regulation of *N. vectensis* MIPs Under Acute Salinity Stress

Next, we sought to evaluate these proteins in individual animals. To understand the role of *N. vectensis* aquaporin and aquaglyceroporin proteins for homeostatic regulation in such variable saline environments, we performed an analysis of the organisms' dynamic, physiological response to salinity fluctuations for each MIP by shifting *N. vectensis* from a 15ppt saline environment to 5ppt, 15ppt, or 35ppt saline environments in both acute and chronic exposures. Quantitative reverse transcription PCR revealed a modulation in the expression of certain aquaporin proteins for *N. vectensis* when exposed to acute changes in salinity for adult stages. The results for acute osmotic shifts in adult stage *N. vectensis* revealed that an increase in salinity resulted in an upregulation of Aqp1 (Fig. 7A) and downregulation of Aqp12 transcription (Fig. 7G). Functional Aqps each exhibited differences in transcription between two groups undergoing opposing conditions of stress (Fig. 7D-F) or between stressed and unstressed organisms (Fig. 7A). A transcriptional difference between stressed and unstressed *N. vectensis* is also noted for Aqp12, but the increase in salinity resulted in a reduction in transcription. An acute decrease in salinity resulted in greater transcription of Aqp4 (Fig. 7D) and Aqp5 (Fig. 7E) when compared to acute and chronic increases in salinity. An acute decrease in salinity for Aqp8 exhibited greater transcription when compared to a chronic increase in salinity (Fig. 7F). There was no significant difference in regulation of Aqp2 or Aqp3 due to acute or chronic osmotic shifts (Fig. 7B-C). This suggests *in vivo*, Aqp1, Aqp4, Aqp5, Aqp8, are significantly modulated in response to different levels of salinity at the organismal level. Interestingly, contrary to our yeast functionality results, we found Aqp12 transcription appears to be active and responsive in its native state.

3.6 Structural Homology Modeling

We used Iterative Threading Assembly Refinement (I-TASSER) protein homology modeling to create structural models for each MIP in order to analyze their structures. Using *E. coli* aquaporin Z (AqpZ) as reference structure, we successfully mapped the solute pore for each MIP using MOLEonline (Fig. 8A) [37]. Clearly visible, at the tightest constriction point, is the selectivity filter (SF) [26,38] (Fig. 8B). SF length and SF diameter are two properties that we define as the SF region of interest, while the hydropathy score of the pore is also depicted (Fig. 8B). These three features were used in a mathematical model which could define a numerical threshold for functionality corresponding with yeast growth assay data displayed in far-right column of Figure 8C. The relative contribution of each SF property to the overall functionality of the pore can be compared. All nonfunctional MIPs generated values universally less amenable to water transport as compared to functional MIPs using this mathematical model.

CHAPTER 4: DISCUSSION

4.1 *N. vectensis* MIP Functional Variability in Yeast.

Our study provides insights into the *in vivo* functionality of seven MIPs identified in *N. vectensis.* Using phylogenetics we identified 8 putative *N. vectensis* MIPs and successfully demonstrated 4 of these were functional in transport in budding yeast (Fig. 3). Furthermore, transcriptional analysis of the MIPs in individual *N. vectensis* animals further support our functional analysis in yeast, demonstrating Aqp1, Aqp4, Aqp5, Aqp8, mRNA transcripts are differentially regulated during environmental osmotic variation. Moreover, nonfunctional Aqp2 and Aqp3 in yeast exhibited no significant differences in overall expression. While Aqp12 transcription did respond to osmotic variation, it was the only MIP that exhibited a reduction in expression compared to unstressed organisms, suggesting a minor role in water homeostasis. However, determining the molecular mechanism underlying the varying phenotypes we observed in our yeast assays was not clear. We evaluated *N. vectensis* MIP protein expression both biochemically and via live-cell fluorescence microscopy, but found no clear relationship between strains with functional phenotypes and level of protein expression and/or subcellular localization.

While our MIP yeast growth assays demonstrate a clear pattern of functionality for Aqp1, Aqp4, Aqp5, and Aqp8 phenotypes, each reducing cell fitness when heterologously expressed in yeast. Aqp2, Aqp3, Aqp12 displayed no detectable decrease in cell fitness, indicating these MIPs are nonfunctional. While each MIP was cloned into centromeric vectors with constitutive CPY promoters, we hypothesized slight variable expression or degradation may be masking functionality. Statistical analysis revealed that there were differences in overall levels of protein expression between strains, but there was no clear correlation between level of expression and reduced functionality. Of the MIP variability in expression, nonfunctional Aqp12 expression

was the lowest, suggesting protein abundance may play a role in Apq12 lack of functionality in yeast. However, Aqp8 was also one of the lowest expressing MIP in yeast and displayed functionality. Likewise, Aqp2 and Aqp3 also expressed well in yeast but did not display a functional phenotype (Fig. 5). A similar study using human aquaporin proteins expressed in yeast also found a high degree of variability in expression levels of these MIPs and arrived at a similar conclusion, though hypothesized MIP oligomerize may also be a factor [27].

Next, we visualized each *N. vectensis* MIP as GFP fusion proteins in yeast using fluorescence deconvolution microscopy. Our rationale for this was that MIP expression, stability, or protein targeting to the plasma membrane can potentially be altered by a single point mutation [41]. Live-cell fluorescence microscopy allowed us to visualize and track in real-time the subcellular localization of these proteins. We defined proper protein targeting by MIP localization to organelles of the endomembrane system such as the endoplasmic reticulum (ER), golgi, endosome, vacuole or plasma membrane. Surprisingly, each *N. vectensis* MIP successfully localized to the plasma membrane and other endomembrane compartments, indicating subcellular localization is not a factor in their functionality.

4.2 Protein Structure Homology Modeling Reveal Key MIP properties.

While expression analysis and subcellular localization studies failed to identify a functional correlation for *N. vectensis* MIPs, we hypothesized their protein structures could reveal key biophysical features that could dictate and predict functionality. Previously, the subatomic structures of Aqps and Glps were solved using X-ray crystallography [26]. These structures provided us with a high-resolution template to determine the structure and function for MIPs in *N. vectensis*.

We found each variable did not independently correlate with MIP functionality. For example, Aqp2 had relatively normal hydropathy and SF length, however, it had a small 0.2 Å SF, which is predicted to be ~9X smaller than that of AqpZ, suggesting the pore size is too small for water to transport. While low expression levels may partially explain Aqp12's nonfunctionally, it also had one of the smallest predicted SF radii and had nonfunctional values for SF length and hydropathy. Aqp3 models predicted nonfunctional scores in both SF length and hydropathy value, though had normal SF radius, suggesting a combination of these variables is critical. Here, we theorize general guidelines for determining the ability of MIPs to facilitate water through their transmembrane pores using increased radius, reduced length, and a smaller hydropathy to predict functionality. Therefore, taking these three variables into account, we hypothesize that we can accurately predict MIP functionality from protein structure homology modeling data. We quantitatively define this as a numerical score for functionality, by taking the ratio of total hydropathy (H_t) and SF length (L) by SF radius (r) (Fig. 8C).

4.3 Future Directions

Here, we demonstrate a combinational approach to characterize and identify MIPs in *N. vectensis*. Our *in vivo* and *in vitro* studies identified 4 functional MIPs, however, failed to reveal a definitive correlation between functional and nonfunctional MIPs. However, using an *in silico* approach based on protein structure we believe functionality can be predicted using a ratio of hydropathy and SF length. This approach would be extremely beneficial to how future studies are designed to determine MIP functionality in nonstandard model organisms such as *N. vectensis*. Our data demonstrated a structural biology approach paired with a functional yeast study can be used to expedite and potentially eliminate the necessity in performing timely and costly experiments such as X-ray crystallography.

However, it is also important to note that some aquaporins rely on other regulatory mechanisms to function. Mammalian Aqp5 has been previously expressed in yeast and was revealed to be regulated by extracellular pH [42]. Therefore, developing structural homology models, though informative, lack in vivo regulatory differences between the MIPs.

In order to develop a higher understanding of MIP function in tissue grade organisms, we need to further study each of the MIPs at the organismal level. One way is to use CRISPR/Cas to analyze these proteins in *N. vectensis* [43]. CRISPR-mediated DNA deletion (or insertion) into the genome is permanent and highly specific, minimizing the cell heterozygosity observed in traditional stable expression technologies that rely on random chromosomal integration. Introducing point indels into the first exon of each MIP, we can generate knockout individuals and phenotypes that can be characterized morphologically through visual observation and *in situ* hybridization with developmental markers [44]. It is possible that deletions of functional MIPs are lethal, if so, we can also partially suppress expression using morpholinos [44,45]. Similarly, we plan to introduce fluorescent epitopes tags to *N. vectensis* MIPs to evaluate the localization of these proteins in embryos, larvae, and adults under variable salinity. We can also manipulate the animal's abiotic gas, temperature and media conditions and use time-lapse video to elucidate the precise trafficking conditions that allow for MIP localization. We also plan to use site directed mutagenesis to alter the properties of the pore and to create functional gain or loss mutants based on our theorized guidelines for MIP functionality. This approach would further validate our guidelines which can then be used to expedite future investigations.

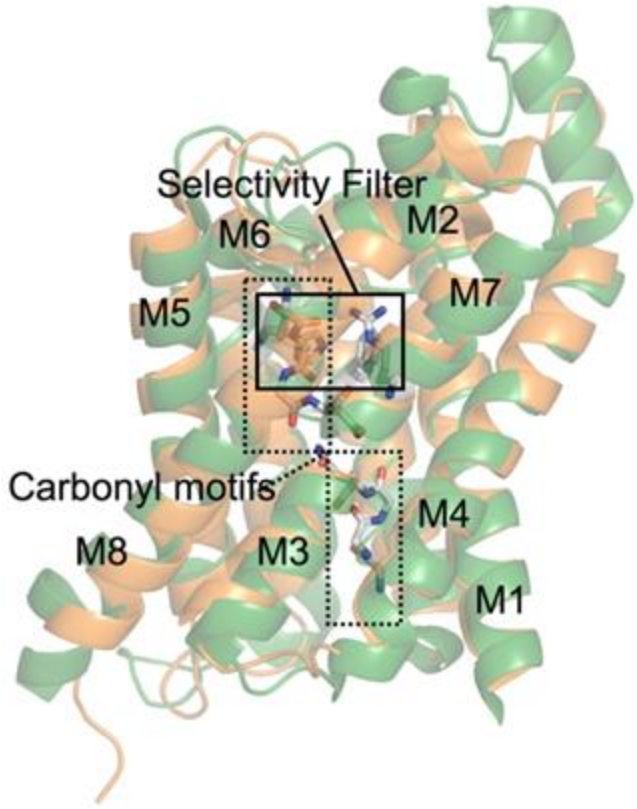

Figure 1. Superposition of *E. coli* AqpZ (orange) and GlpF (green) monomer ribbon structures. M1-M8 represent helices with dashed boxes showing symmetry related carbonyls and solid boxes indicate the selectivity filter in the channel pore [23].

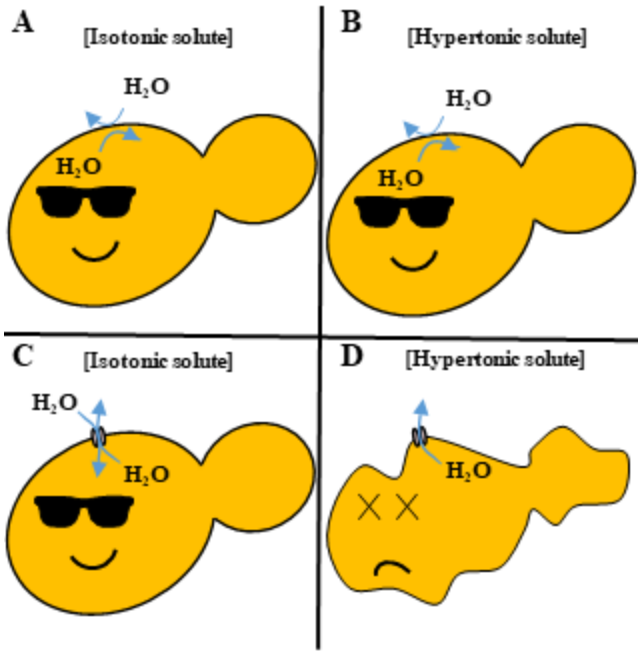

Figure 2. Osmotic stress in yeast. (A) and (B) show WT yeast in isotonic and hypertonic salinity with no functional foreign MIPs. (C) and (D) show yeast expressing functional foreign MIPs in isotonic and hypertonic environments. High solute results in cell death.

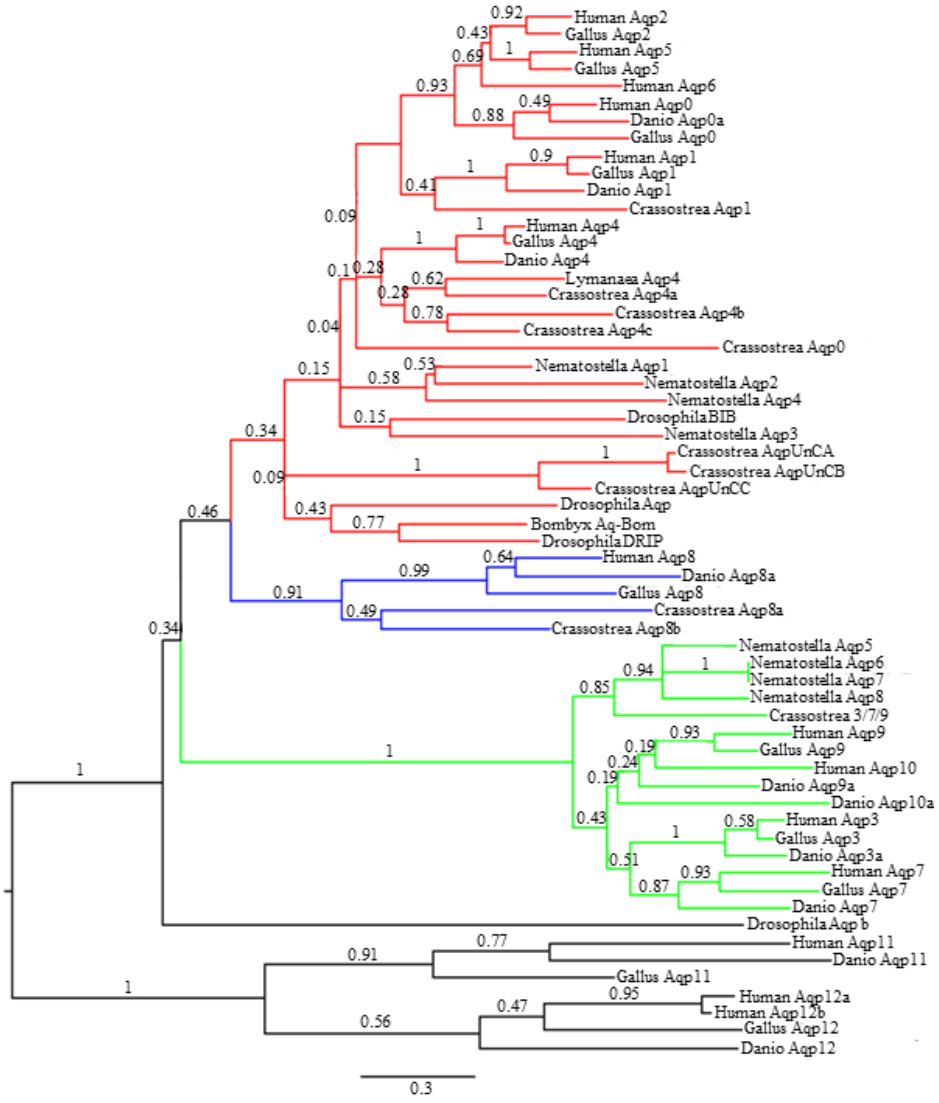

Figure 3. Phylogenetic analysis of MIPs. Phylgenetic tree indicates three clades: aquaporin 1-like classical aquaporin (red), aquaporin 8 (blue) and aquaporin 3-like aquaglyceroporins (green). There are four *N. vectensis* MIPs in the classical aquaporin clade and four in the aquaporin 3-like aquaglyceroporin clade.

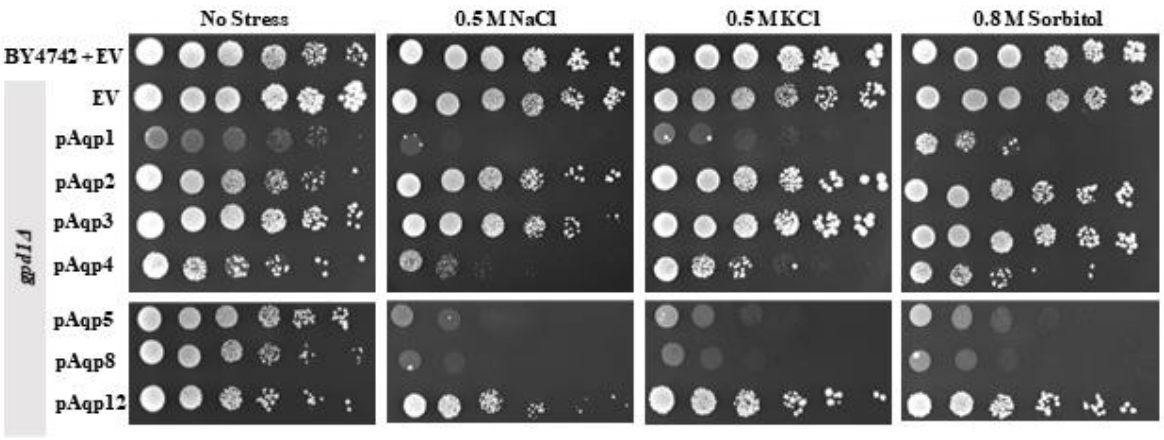

Figure 4. *N. vectensis* MIP yeast growth assay. Strains expressing *N. vectensis* MIPs were grown in dropout media containing no stress, 0.5 M NaCl, 0.5 M KCl, or 0.8 M Sorbitol. Wildtype (BY4742) or *gpd1Δ* expressing empty vector(EV) were used as controls. Varying degrees of reduced cell fitness was observed for strains expressing Aqp1, Aqp4, Aqp5, and Aqp8 MIPs in each stress condition.

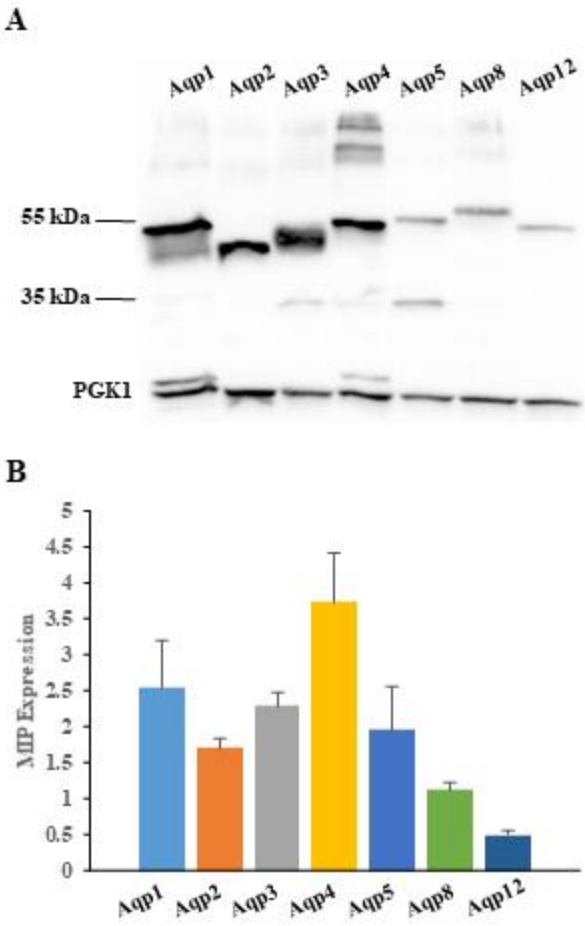

Figure 5. Quantitative western blot analysis of *N. vectensis* MIP expression in *S. cerevisiae*. (A) Western blot of indicated *N. vectensis* MIPs. Proteins were detected using anti-GFP (B) Graph of densitometry analysis. The ratio of band intensities of each MIP and corresponding PGK1 load were calculated and averaged using data from 3 experiments.

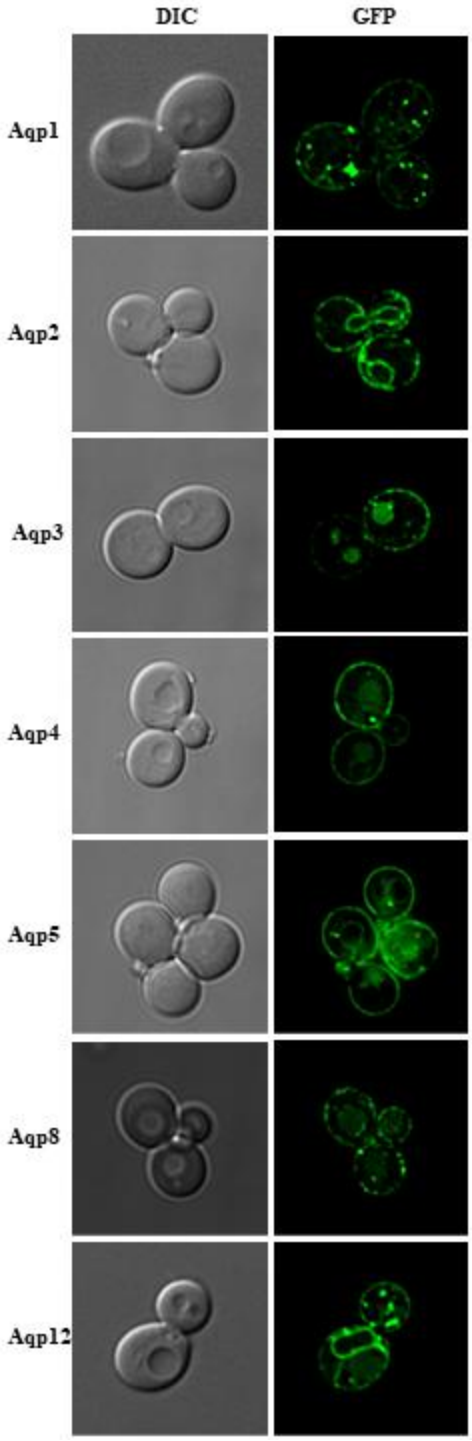

Figure 6. Subcellular localization of MIPs in *S. cerevisiae.* C-terminal GFP fusion proteins were expressed on plasmids in BY4742 yeast strains and visualized at log-phase. Left: Differential interferences contrast images, right: fluorescent images. Note that all strains exhibit some degree of PM localization.

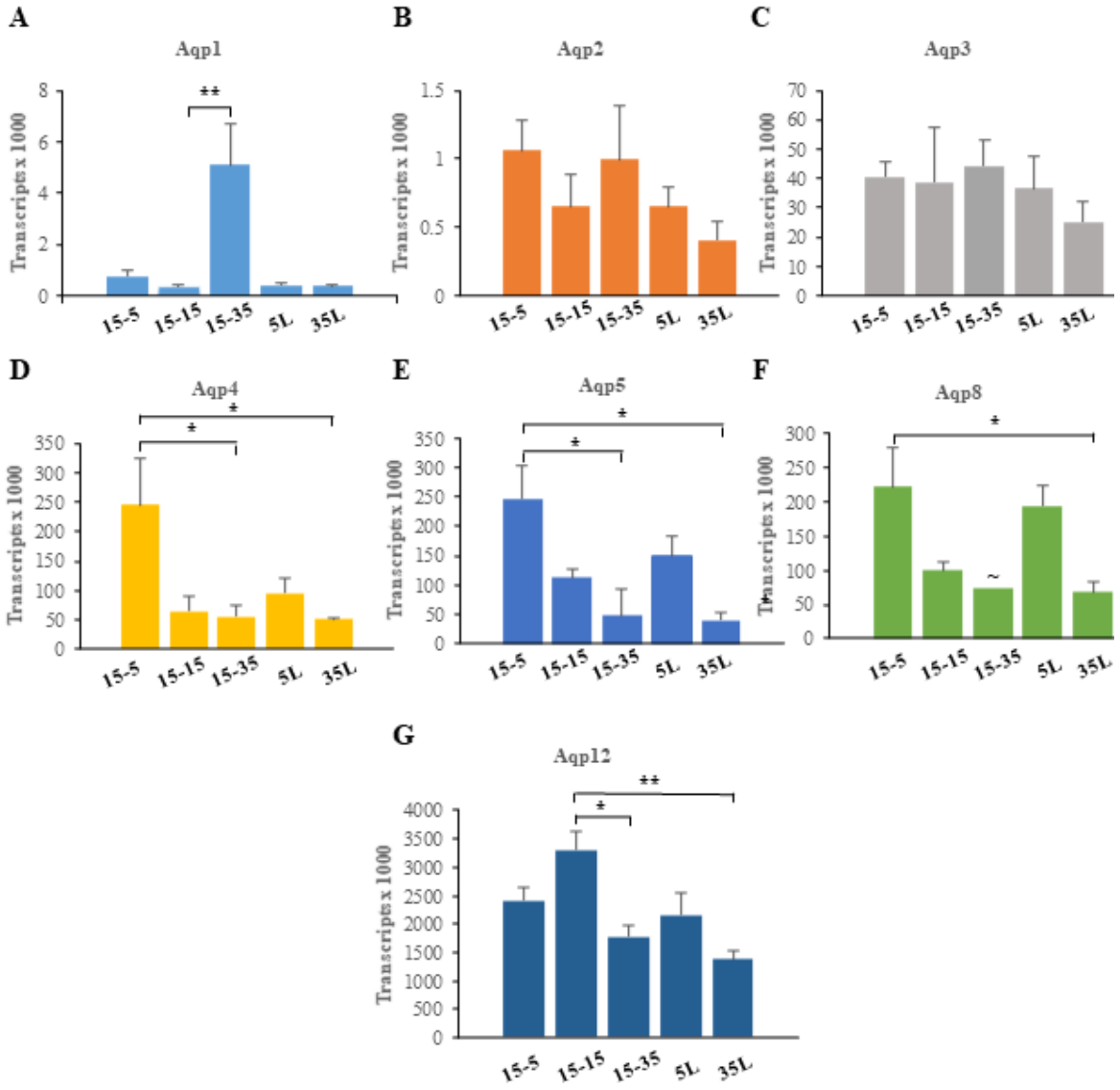

Figure 7. Transcriptional Regulation of *N. vectensis* classical aquaporins in osmotic stress. A-G represent Aqp1, Aqp2, Aqp3, Aqp4, Aqp5, Aqp8 and Aqp12 respectively. Initially grown in 15ppt salinity, acute shifts in salinity were measured at 5ppt (15-5), 15ppt (15-15), and 35ppt (15-35) salinity conditions. Chronic shifts to 5ppt (5L) and 35ppt (35L) salinity were also measured. The relative shift in overall transcription of each MIP was recorded and displayed with "*" indicating statistical significance between relevant groups and "~" noting the absence of replicates.

A

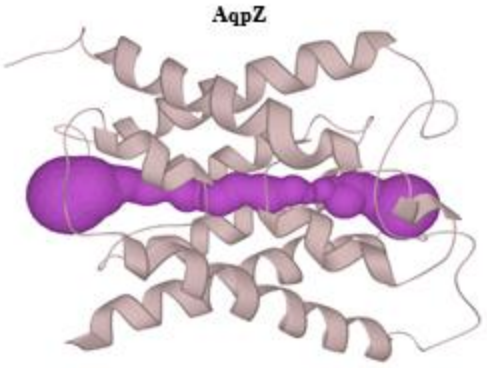

B

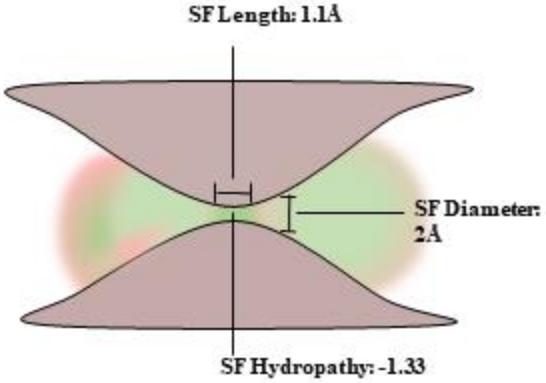

C

MIPs	H_A	Radius	Length	$\frac{L+(H_A-H_Z)}{r}$
AqpZ				
Aqp1				
Aqp2				
Aqp3				
Aqp4				
Aqp5				
Aqp8				
Aqp12				

Figure 8. Homology Models of *N. vectensis* MIPs. (A) Ribbon diagram of *E. coli* AqpZ with solute pore modeled (purple) (B) Cartoon model of example AqpZ pore. Selectivity Filter (SF) length, diameter, and hydropathy are indicated. Degree of hydropathy is depicted using green (low hydropathy) and red (high hydropathy). (C) Summary heat map of pore properties of *N. vectensis* MIPs. Shades of green and red indicate degrees of functionality.

Gene	Amplicon	Forward (5-3)	Reverse (5-3)
Aqp1	Clone-qPCR	TTCTACGGGGAGCGTTCTAC	CTTATCCACAGGCGTCAGC
	qPCR	GCGGTTATCATGAATATCTGGAC	TGGTAGAGCAGGGAAGCAAG
	Full length	GTGAAAAGCGTGCGAAACTC	GATAATCTAGTTTTCCTATGGTA CTCG
	Yeast expression	GGGGACAAGTTTGTACAAAAAAGCAGGCTTA ATGTTCCTTAGAGAATTTCTAACCGGGAA	GGGGACCACTTTGTACAAGAAAG CTGGGTTATGGAGTTCCACATCT TCTGGG
Aqp2	Clone-qPCR	TGTTCCTTGTCTGTGCAAGC	GACCGTGCAGGGTTCATACT
	qPCR	TGCATGGTTTGGTGTTTGTG	ACGGTGTCAGTCCGAATAGG
	Full length	AAGCAACTCTTCATCGGCGCTCT	TTACCAGTGATGTCTCCAGTGAT CCAT
	Yeast expression	GGGGACAAGTTTGTACAAAAAAGCAGGCTTA ATGAAGCAACTCTTCATCGGCG	GGGGACCACTTTGTACAAGAAAG CTGGGTTCCAGTGATGTCTCCAG TGATCCAT
Aqp3	Clone-qPCR	TACTTGGGCACGCTTCTCTT	CCCACACCAGTAAACCCAGT
	qPCR	TGTGGCGTCATTTCTTTACG	GCAGGGCACACTAGATGGAG
	Full length	TTTGTCGCTACGCACAAGTC	TTGTGCGGTACATGAAATCG
	Yeast expression	GGGGACAAGTTTGTACAAAAAAGCAGGCTTA ATGGTTCACTTCAGGAGACTAAAAGT	GGGGACCACTTTGTACAAGAAAG CTGGGTTAGGGCTCAACTCTTCG GTATCG
Aqp4	Clone-qPCR	GTGGGACGGCACTACAAAAC	GCGCAAACACATGGTGATAA
	qPCR	CTGGCAAGAAAACACTGCTG	TCCACAGAATGCTGAGATGC
	Full length	CACGCATCTTTTAGCCATTG	TGTCTGATGTAGCCGCGTAG
	Yeast expression	GGGGACAAGTTTGTACAAAAAAGCAGGCTTA ATGATCACGTATTGCGGATTCACC	GGGGACCACTTTGTACAAGAAAG CTGGGTTTAATCGGCAAACATTC GTCTCTTGTCC
Aqp5	Clone-qPCR	ACCCACGGGACTTTCTTCTC	CGAATACCCCAAAAGCAAAA
	qPCR	TAACTTCAGCTGGGGAATGG	CACTACGGCGAATGCTACAG
	Full length	CAGCCTTCAAGAAAGCGAAG	GATAAGAGGACGCCACCAAA
	Yeast expression	GGGGACAAGTTTGTACAAAAAAGCAGGCTTA ATGCCTCGTTGTTCGGTTCA	GGGGACCACTTTGTACAAGAAAG CTGGGTTGATGTGACTCTCCCAT TGTTTTCTCC
Aqp8	Clone-qPCR	CGGGTTTCGACTAAACAAGAG	AATTCTCGTCGCTTGACTGG
	qPCR	GCAAGTTAAAACTCGGGATCAG	TGCGATGAATTCTGCCATAC
	Full length	GAAAGCGGAGGAAGACGAAT	CGCCTCGCGTATATCTTACA
	Yeast expression	GGGGACAAGTTTGTACAAAAAAGCAGGCTTA ATGGCAACTAATCGTTTACGCG	GGGGACCACTTTGTACAAGAAAG CTGGGTTCAAGACAGTCAAATTC TCGTCGCTTGACT
Aqp12	Clone-qPCR	ACCTCACGTGTGGATTTCCT	CTGTTACTTGAAACCTCTCATGC
	qPCR	GGCAAACCCTTGTGGATTAC	GCGCCAGAAAATTGAAAAAG
	Full length	ACCTCACGTGTGGATTTCCT	CTGTTACTTGAAACCTCTCATGC
	Yeast expression	GGGGACAAGTTTGTACAAAAAAGCAGGCTTA ATGGATATCCTATGGTCAGTTGCCG	GGGGACCACTTTGTACAAGAAAG CTGGGTTGCGAACACCAGTGCTG GT

Table 1: Primer design. Primers were developed for evaluating transcriptional regulation of MIPs in *N. vectensis* as well as to generate yeast expression vectors for functional analysis, including quantitative assessment and subcellular localization.

REFERENCES

1. Mackas DL, Greve W, Edwards M, Chiba S, Tadokoro K, Eloire D, Mazzocchi MG, Batten S, Richardson AJ, Johnson C, Head E, Conversi A, Peluso T. Changing zooplankton seasonality in a changing ocean: Comparing time series of zooplankton phenology. Progress in Oceanography. 2012;97–100:31-62.
2. Varpe Ø. Fitness and phenology: annual routines and zooplankton adaptations to seasonal cycles. Journal of Plankton Research. 2012. 34:267–276.
3. Wen CK, Almany GR, Williamson DH, Pratchett MS, Jones GP. Evaluating the effects of marine reserves on diet, prey availability and prey selection by juvenile predatory fishes. Marine Ecology Progress Series. 2012;469:133-144
4. Talmage SC, Gobler CJ. Effects of elevated temperature and carbon dioxide on the growth and survival of larvae and juveniles of three species of northwest Atlantic bivalves. PLoS One. 2011;6(10):e26941.
5. Whitehead A, Roach JL, Zhang S, Galvez F. Genomic mechanisms of evolved physiological plasticity in killifish distributed along an environmental salinity gradient. Proceedings of the National Academy of Sciences. 2011;108(15):6193-6198.
6. Brennan RS, Galvez F, Whitehead A. Reciprocal osmotic challenges reveal mechanisms of divergence in phenotypic plasticity in the killifish Fundulus heteroclitus. The Journal of Experimental Biology. 2015;218(8):1212-1222.
7. Ewing RD, Peterson GL, Conte FP. Larval salt gland of Artemia salina nauplii. Journal of Comparative Physiology. 1974;88(3):217-234.

8. Abatzopoulos TJ, El-Bermawi N, Vasdekis C, Baxevanis AD, Sorgeloos P. Effects of salinity and temperature on reproductive and life span characteristics of clonal Artemia. . Hydrobiologia. 2003;492(1):191-199.
9. Reitzel AM, Darling JA, Sullivan JC, Finnerty JR. Global population genetic structure of the starlet anemone *Nematostella vectensis*: multiple introductions and implications for conservation policy. Biological Invasions. 2008;10(8):1197-1213.
10. Hand C, Uhlinger K. The unique, widely distributed sea anemone, *Nematostella vectensis* Stephenson: A review, new facts, and questions. Estuaries. 1994;17(2):501-508.
11. Frank PG, Bleakney JS. Asexual reproduction, diet, and anomalies of the anemone *Nematostella vectensis* in Nova Scotia. Canadian Field Naturalist 1978;92:259-263.
12. Reitzel AM, Chu T, Edquist S, Genovese C, Church C, Tarrant AM, Finnerty JR. Physiological and developmental responses to temperature by the sea anemone *Nematostella vectensis*. Marine Ecology Progress Series. 2013;484:115-130.
13. Putnam NH, Srivastava M, Hellsten U, Dirks B, Chapman J, Salamov A, Terry A, Shapiro H, Lindquist E, Kapitonov VV, Jurka J, Genikhovich G, Grigoriev IV, Lucas SM, Steele RE, Finnerty JR, Technau U, Martindale MQ, Rokhsar DS. Sea anemone genome reveals ancestral eumetazoan gene repertoire and genomic organization. Science. 2007;317(5834):86-94.
14. Helm RR, Siebert S, Tulin S, Smith J, Dunn CW. Characterization of differential transcript abundance through time during *Nematostella vectensis* development. BMC Genomics. 2013;14:266.

15. Schwaiger M, Schönauer A, Rendiro AF, Pribitzer C, Schauer A, Gilles AF, Schinko JB, Renfer E, Fredman D, Technau U. Evolutionary conservation of the eumetazoan gene regulatory landscape. Genome Research. 2014: 24: 639-650.
16. Hand C, Uhlinger KR. The culture, sexual and asexual reproduction, and growth of the sea anemone *Nematostella vectensis*. The Biological Bulletin. 1992;182(2):169-176.
17. Hand C, Uhlinger KR. Asexual reproduction by transverse fission and some anomalies in the sea anemone *Nematostella vectensis.* Invertebrate Biology. 1995;114(1):9-18.
18. Zamer WE, McManus MG, Rowell CB. Physiological variation in clonal anemones: energy balance and quantitative genetics. American Zoologist. 1999;39:412-421.
19. Shick JM, Hoffmann RJ, Lamb AN. Asexual reproduction, population structure, and genotype-environment interactions in sea anemones. American Zoologist. 1979;19(3):699-713.
20. Shick JM, Dowse HB. Genetic basis of physiological variation in natural populations of sea anemones: intra- and interclonal analyses of variance. In: Gibbs PE, editor. Proceedings of the 19th European Marine Biology Symposium. Cambridge: Cambridge University Press; 1985. p. 165-179.
21. Schäffner AR. Aquaporin function, structure, and expression: are there more surprises to surface in water relations? 1998;204(2):131-139
22. Abascal F, Irisarri I, Zardoya R. Diversity and evolution of membrane intrinsic proteins. Biochimica et Biophysica Acta. 2014;1840(5):1468-1481.
23. Savage, D., O'Connell J., Miercke, L., *et al.* Structural context shapes the aquaporin selectivity filter. 2010; 107(40):17164-17169

24. Finn RN, Chauvigné F, Hildberg JB, Cutler CP, Cerdà J. The Lineage-Specific Evolution of Aquaporin gene Clusters Facilitated Tetrapod Terrestrial Adaptation
25. Kosicka E, Grobys D, Kmita H, Lesicki A, Pieńkowska JR. Putative new groups of invertebrate water channels based on the snail *Helix pomatia* L. (Helicidae) MIP protein identification and phylogenetic analysis. European Journal of Cell Biology. 2016;95(12):543-551.
26. Finn RN, Cerdà J. Evolution and functional diversity of aquaporins. The Biological Bulletin. 2015;229(1):6-23
27. Pettersson N, Hagstrom J, Bill R, Hohmann S. Expression of heterologous aquaporins for functional analysis in *Saccharomyces cerevisiae*. 2006; 1(50): 247-255
28. Bonhivers M, Carbrey JM, Gould SJ, Agre P. Aquaporins in *Saccharomyces*. Genetic and functional distinctions between laboratory and wild-type strains. Journal of Biological Chemistry. 1998;273(42):27565-27572.
29. Albertyn J, Hohmann S, Thevelein JM, Prior BA. GPD1, which encodes glycerol-3-phosphate dehydrogenase, is essential for growth under osmotic stress in *Saccharomyces cerevisiae*, and its expression is regulated by the high-osmolarity glycerol response pathway. Molecular and Cellular Biology 1994;14(6):4135-4144.
30. Pahlman AK, Granath K, Ansell R, Hohmann S, Adler L. The yeast glycerol 3-phosphatases Gpp1p and Gpp2p are required for glycerol biosynthesis and differentially involved in the cellular responses to osmotic, anaerobic, and oxidative stress. Journal of Biological Chemistry. 2001;276(5):3555-3563.
31. Sleator RD, Walsh P. An overview of *in silico* protein function prediction. Archives of Microbiology. 2010; 192:151-155

32. Calvanese L, Pellegrini-Calace M, Oliva R. *In silico* study of human aquaporin AQP11 and AQP12 channels. Protein Science. 2013;22(4): 455-466

33. Winston F, Dollard C, Ricupero-Hovasse SL. Construction of a set of convenient *Saccharomyces cerevisiae* strains that are isogenic to S288C. Yeast. 1995;11(1):53-55.

34. Longtine MS, Mckenzie A, Dermarini DJ, Shah NG, Wach A, Brachat A, Philippsen P, Pringle JR. Additional modules for versatile and economical PCR-based gene deletion and modification in *Saccharomyces cerevisiae*. Yeast. 1998;14(10):953-961.

35. Alberti S, Gitler AD, Lindquist S. A suite of Gateway® cloning vectors for high-throughput genetic analysis in *Saccharomyces cerevisiae*. Yeast. 2007;24(10):913-919.

36. Untergasser A. "Cloning – Gateway BP-Reaction II" Untergasser's Lab. Summer 2006.

37. Reitzel AM, Tarrant AM. Nuclear receptor complement of the cnidarian *Nematostella vectensis*: phylogenetic relationships and developmental expression patterns. BMC Evolutionary Biology. 2009;9:230

38. J Yang, R Yan, A Roy, D Xu, J Poisson, Y Zhang. The I-TASSER Suite: Protein structure and function prediction. Nature Methods. 2015; 12(1):7-8

39. Pravda L., Sehnal, D., Toušek D., *et al.* MOLEonline: a web-based tool for analyzing channels, tunnels and pores (2018 update). 2018; 46(W1): W368-W373

40. Bomholt J, Helix-Nielsen C, Scharff-Poulsen P, Pedersen PA. Recombinant production of human Aquaporin-1 to an exceptional high membrane density in *Saccharomyces cerevisiae*. PLoS One. 2013;8(2):e56431.

41. Lagrée V, Pellerin I, Hubert J, Tacnet F, Cahérec F, Roudier N, Thomas D, Gouranton J, Deschamps S. A yeast recombinant aquaporin mutant that is not expressed or mistargeted in *Xenopus* oocyte can be functionally analyzed in reconstituted proteoliposomes

42. Trodrigues C, Mósca AF, Martins AP, Nobre T, Prista C, Antunes F, Gasparovic AC, Soveral G. Rat aquaporin-5 is pH-Gated induced by phosphorylation and is implicated in oxidative stress. International Jouranl of Molecular Sciences. 2016;17(12):2090
43. Ikmi A, McKinney SA, Delventhal KM, Gibson MC. TALEN and CRISPR/Cas9-mediated genome editing in the early-branching metazoan Nematostella vectensis. Nature Communications. 2014;5:5486.
44. Magie C, Daly M, Martindale M. Gastrulation in the cnidarian Nematostella vectensis occurs via invagination not ingression. Developmental Biology. 2007;305(2):483-497.
45. Rentzsch F, Fritzenwanker J, Scholz C, Technau U. FGF signalling controls formation of the apical sensory organ in the cnidarian Nematostella vectensis. Development. 2008;135(10):1761-1769